Journal of Organometallic Chemistry, 320 (1987) 363–384
Elsevier Sequoia S.A., Lausanne – Printed in The Netherlands

ELECTRON TRANSFER IN ORGANOMETALLIC CLUSTERS

XI *. REDOX CHEMISTRY OF $M_3(CO)_{12}$ (M = Ru, Os) AND PPh_3 DERIVATIVES; MECHANISM OF CATALYSED NUCLEOPHILIC SUBSTITUTION

ALISON J. DOWNARD, BRIAN H. ROBINSON *, JIM SIMPSON

Department of Chemistry, University of Otago, P.O. Box 56, Dunedin, (New Zealand)

and ALAN M. BOND

Division of Chemical and Physical Sciences, Deakin University, Waurn Ponds 3217, Victoria (Australia)

(Received September 3rd, 1986)

Summary

The generality of a two-electron reduction process involving an $\vec{E}C\vec{E}$ mechanism has been established for $M_3(CO)_{12}$ and $M_3(CO)_{12-n}(PPh_3)_n$ (M = Ru, Os) clusters in all solvents. Detailed coulometric and spectral studies in CH_2Cl_2 provide strong evidence for the formation of an 'opened' $M_3(CO)_{12}^{2-}$ species the triangulo radical anions $M_3(CO)_{12}^{-\cdot}$ having a half-life of $< 10^{-6}$ s in CH_2Cl_2. However, the electrochemical response is sensitive to the presence of water and is concentration dependent. An electrochemical response for "opened" $M_3(CO)_{12}^{2-}$ is only detected at low concentrations $< 5 \times 10^{-4}$ mol dm^{-3} and under drybox conditions. The electroactive species found at higher concentrations and in the presence of water $M_3(CO)_{11}^{2-}$ and $M_6(CO)_{18}^{2-}$ were confirmed by a study of the electrochemistry of these anions in CH_2Cl_2; $HM_3(CO)_{11}^-$ is not a product. The couple $[M_6(CO)_{18}]^{-/2-}$ is chemically reversible under certain conditions but oxidation of $HM_3(CO)_{11}^-$ is chemically irreversible. Different electrochemical behaviour for $Ru_3(CO)_{12}$ is found when [PPN][X] ($X = OAc^-$, Cl^-) salts are supporting electrolytes. In these solutions formation of the ultimate electroactive species $[\mu\text{-}C(O)XRu_3(CO)_{10}]^-$ at the electrode is stopped under CO or at low temperatures but $Ru_3(CO)_{12}^{-\cdot}$ is still trapped by reversible attack by X presumably as $[\eta^1\text{-}C(O)XRu_3(CO)_{11}]^-$. It is shown that electrode-initiated electron catalysed substitution of $M_3(CO)_{12}$ only takes place on the electrochemical timescale when M = Ru, but it is slow, inefficient and non-selective, whereas BPK-initiated nucleophilic substitution of $Ru_3(CO)_{12}$ is only specific and fast in ether solvents particularly THF. Metal–metal bond cleavage is the most

* For part X see ref. 1.

0022-328X/87/$03.50

important influence on the rate and specificity of catalytic substitution by electron or [PPN]-initiation. The redox chemistry of $M_3(CO)_{12}$ clusters (M = Fe, Ru, Os) is a consequence of the relative rates of metal–metal bond dissociation, metal–metal bond strength and ligand dissociation and in many aspects resembles their photochemistry.

Introduction

Early electrochemical and ESR studies [2] of $Ru_3(CO)_{12}$ and $Os_3(CO)_{12}$ in acetone indicated that the lifetimes of the radical anions, $M_3(CO)_{12}^{-\cdot}$ are very short. Nonetheless, it has been shown [3,4] that $Ru_3(CO)_{12}$ is a good substrate for electron-initiated catalysed reactions. This contradicts the reasonable premise that suitable substrates for ETC (electron transfer chain) catalysed reactions are those which exhibit reversible or quasi-reversible electrochemical behaviour with respect to the couple [substrate]$^{0/-1}$. Recently Rieger and co-workers have suggested [5], based on the electrochemistry of $Ru_3(CO)_{12}$ in acetone, that an $\vec{ECE}$ process is responsible for the irreversible electron transfer. In this paper we present our results on the redox chemistry $M_3(CO)_{12}$ (M = Ru, Os) and $M_3(CO)_{12-n}(PPh_3)_n$ ($n = 1$–3) in several solvents and supporting electrolytes. Mechanisms of catalysed nucleophilic substitution reactions of $M_3(CO)_{12}$ are also investigated. Preliminary results have been given elsewhere [6].

Results

Potential data are given in Tables 1 and 2.

Electrochemistry of $M_3(CO)_{12}$ in CH_2Cl_2/TBAP

DC polarograms of $M_3(CO)_{12}$ (M = Ru, Os) recorded under CO were identical to those under Ar and consisted of a single wave for which $\log[i/(i_d - i)]$ vs. E gave a slope of ~ 60 mV for values of $i < 75\%\ i_d$. Distortion of the wave slopes near the limiting current region were observed at all concentrations and drop times. Other parameters (linear dependence of i_d on concentration, $i_d \propto h$) show that the waves are diffusion-controlled and therefore, on this timescale, any chemical steps preceding charge-transfer are not rate-controlling. In order to establish n, diffusion currents of the known [2,7] one-electron couple $[Fe_3(CO)_{12}]^{0/-}$ were compared with those of $Ru_3(CO)_{12}$ at the same concentration under the same electrochemical conditions. Values of $n = 1.8$, 1.9 (M = Ru) and $n = 2.0$, 2.0 (M = Os) were obtained from dc and pulse experiments respectively, confirmed by the coulometric data discussed below.

The voltammetric responses of $Ru_3(CO)_{12}$ and $Os_3(CO)_{12}$ were not dependent on the scan rate but were sensitive to the concentration of substrate and water.

Cyclic voltammograms of $M_3(CO)_{12}$ at Pt and glassy carbon electrodes were recorded at scan rates of 0.05–1.0 V s^{-1} using conventionally-sized electrodes and at faster scan rates (50–10^4 V s^{-1}) using a Pt microelectrode of 10 μm diameter. The peak potentials are dependent on scan rate but in all experiments an irreversible two-electron process is observed at E_{pc} in the range $-0.95 \rightarrow -1.4$ V depending on scan rate, and an irreversible oxidation process at $E_{pa} \sim 1.4$ V. The current

TABLE 1

ELECTROCHEMICAL DATA FOR $M_3(CO)_{12}$ [a]

Solvent	Electrolyte	DC Polarography [b]		Cyclic voltammetry [c]		
		Reduction		Reduction		Oxidation
		$E_{1/2}$ (V)	$E_{1/4}-E_{3/4}$ (V)	E_{pc} (V)	E_{pa} (V)	E_{pa} (V)
M = Ru						
CH_2Cl_2	TBAP	−0.97	60	−1.00	−0.45 0.36	1.42
	PPNOAc	–	–	−1.10	−0.06	–
	$PPNClO_4$	−0.97	100	−1.16	−0.50 0.39	–
	PPNCl	–	–	−1.09 (−0.73) [d]	–	–
	$PPNClO_4/OH^-$ [e]	−0.96	90	−1.16	−0.10	–
THF [f]	TBAP	−0.85	140	−0.98 −1.23	−0.47	–
acetone	TEAP	−0.91	110	−1.05	−0.43	1.20
CH_3CN	TEAP	−1.00	70	−0.82 −1.19	−0.32	–
M = Os						
CH_2Cl_2	TBAP	−1.31	60	−1.54	−0.24 −0.04	1.54
	PPNX [h]	−1.36 [g]	90	−1.52	−1.4	–
THF	TBAP	−1.12	70	−1.28	−0.46 −0.09	–

[a] Volts vs. Ag/AgCl at 293 K. [b] Drop time 0.5 s; scan rate 10 mV s^{-1}. [c] At Pt, scan rate 200 mV s^{-1}. [d] On repeat scans only. [e] as n-$Bu_4N^+ OH^-$. [f] $i-E$ responses were erratic; results given are most consistent. [g] $X^- = ClO_4^-$. [h] E_{pc} independent of X^-.

function for the reduction step ($i_{pc}/v^{1/2}$) decreases with increasing sweep rate consistent with slow electron-transfer kinetics.

Other oxidation processes follow scan reversal beyond the two-electron reduction step but the precise profile on the anodic scan is dependent on the cluster, on the condition of the electrode, on the scan rate, but more specifically, on the substrate concentration and the presence of water.

Reproducible profiles are found when the electrochemical work is carried out in a dry box with low concentrations of $Ru_3(CO)_{12}$ ($\sim 1 \times 10^{-4}$ mol dm^{-3}) (Fig. 1a) at scan rates up to 1 V s^{-1}. In this case the dominant oxidation wave [8] is at ~ -0.6 V (**D**) with a peak current $\sim 75\%$ of the reduction wave and a well-defined $t^{-1/2}$ decay.

Under drybox conditions at higher concentrations of $Ru_3(CO)_{12}$ wave **D** disappears to be replaced by wave **B** (Fig. 1c) which does not have $t^{1/2}$ shape. A very small feature **C** also appears which is independent of the primary electrode process as it is chemically reversible under drybox conditions. At this point we note that wave **C** is due to the oxidation of $Ru_6(CO)_{18}^{2-}$ as suggested by Rieger and

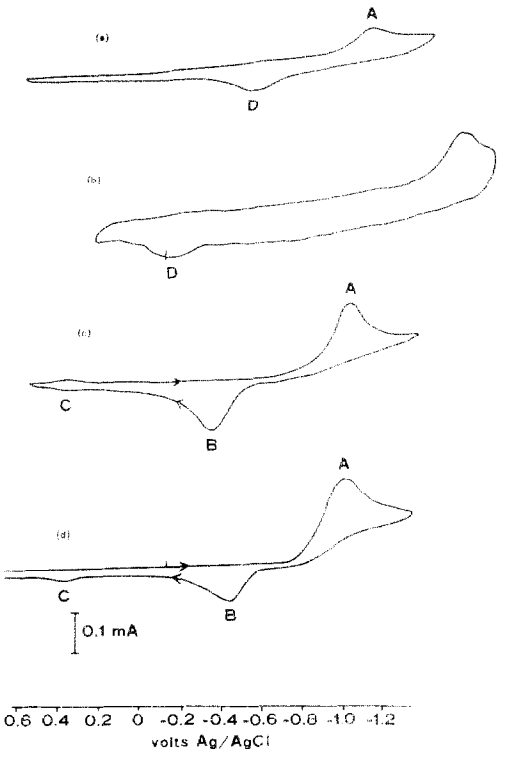

Fig. 1. Cyclic voltammograms of $Ru_3(CO)_{12}$ in CH_2Cl_2. (a) dry-box/N_2, $[Ru_3(CO)_{12}]$ 1.2×10^{-4} mol dm^{-3}, 293 K, 200 mV s^{-1} glassy carbon electrode, 0.1 mol dm^{-3} TBAP. (b) $[Ru(CO)_{12}]$ 3×10^{-3} mol dm^{-3}, under Ar, Pt microelectrode, 5000 V s^{-1} 0.5 mol dm^{-3} $TBABF_4$, 293 K. (c) dry-box/N_2, $[Ru_3(CO)_{12}]$ 2.8×10^{-3} mol dm^{-3}, 200 mV s^{-1}, 0.1 mol dm^{-3} TBAP, glassy carbon electrode. (d) under Ar, 'normal' laboratory conditions, $[Ru_3(CO)_{12}]$ 1×10^{-3} mol dm^{-3}, 200 mV s^{-1} 0.1 mol dm^{-3} TBAP, Pt.

co-workers [5], produced by a reaction between $Ru_3(CO)_{12}$ and $Ru_3(CO)_{11}^{2-}$ (vide infra).

Significant differences occur when the scans for $Ru_3(CO)_{12}$ are run without rigorous exclusion of water and at substrate concentrations, 5×10^{-4} mol dm^{-3}. Figure 1d shows a cyclic voltammogram typical of those recorded at 0.05–0.5 V s^{-1}. Wave **C** is still small but it is no longer chemically reversible; the peak current variation with scan rate is consistent with the effects of diffusion alone (that is, the species giving rise to this wave, $Ru_6(CO)_{18}^{2-}$, is stable on the electrochemical timescale). In contrast, the wave at ~ -0.45 V (**B**) is markedly scan rate dependent, the current decreasing rapidly with decreasing scan rate, suggesting that this species is unstable on this timescale. On Hg, the feature around -0.45 V on the oxidation scan has the appearance of a 'doublet': the second component has an E_{pc} of ~ -0.6 V corresponding to wave **D**. Clearly, Hg is not an 'innocent' electrode and could be stabilising the anionic species giving rise to wave **D**.

Scans at rates between 1–50 V s^{-1}, concentration $> 5\times10^{-4}$ mol dm^{-3} show the three oxidation waves **B**, **C**, **D** with progressive decrease in i_{pc} of **B** and **C** with increasing scan rate. Only one oxidation wave is seen at scan rates between 50 and

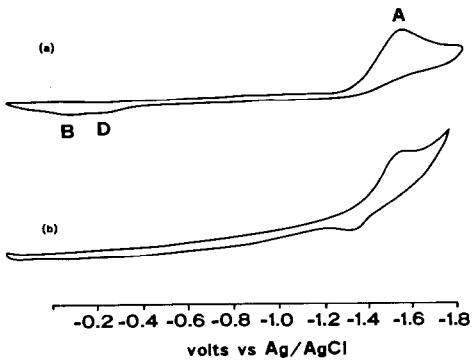

Fig. 2. Cyclic voltammograms of $Os_3(CO)_{12}$ in CH_2Cl_2 at 200 mV s^{-1}. (a) $[Os_3(CO)_{12}]$ 1×10^{-3} mol dm^{-3}, TBAP (0.1 mol dm^{-3}). (b) $[Os_3(CO)_{12}]$ 5×10^{-4} mol dm^{-3}, Pt, $[PPN][ClO_4]$ (0.1 mol dm^{-3}).

15000 V s^{-1} on a microelectrode and, while the large IR effects make a correlation with the i–E responses at slower rates difficult, it is consistent with an assignment to wave **D** (the slow electrode kinetics causes a shift of over 0.5 V in both **A** and **D** at 5000 V s^{-1} compared with potentials at 200 mV s^{-1}, Fig. 1b).

A two-electron chemically irreversible reduction wave also characterises the cyclic voltammograms of $Os_3(CO)_{12}$ (Fig. 2). Under dry-box conditions and at low concentrations the oxidation response is very similar to that of $Ru_3(CO)_{12}$ with a single wave of relatively low i_{pa} at ~0.7 V (**D**). Under 'normal' conditions two small oxidation waves (**B&C**) are observed and the overall profile is the same under CO or Ar and at 293 or 203 K (Fig. 2a).

Clearly both $Ru_3(CO)_{12}$ and $Os_3(CO)_{12}$ are involved in electrode processes in which chemical and electrochemical steps follow the initial one-electron reduction to the respective radical anions $M_3(CO)_{12}^{-\cdot}$. These are discussed later.

$$M_3(CO)_{12} + e \rightleftharpoons M_3(CO)_{12}^{-\cdot} \xrightarrow{CE} M_3(CO)_{12}^{2-} \qquad (2)$$

Electrochemistry of $M_3(CO)_{12}$ in the presence of PPN salts in CH_2Cl_2

Kaesz and co-workers have shown [9] that [PPN][X] salts ($X^- = OAc^-$, CN^-, F^- etc.) catalyse the substitution of one or more CO groups by phosphines. This finding and related reactions with PPN salts [10,11], together with the knowledge that the rates of reactions involving cluster radical anions can be influenced by the counter-ion [12], raised the possibility that a gegenion of the supporting electrolyte could be mediating the i–E responses described above for $M_3(CO)_{12}$.

Potentials for the primary reduction process for $M_3(CO)_{12}$ are essentially unaffected by the change from a n-$Bu_4N^+X^-$ to PPN^+X^- supporting electrolyte (Table 1) and with $[PPN][ClO_4]$ the characteristic two-electron reduction wave with a diffusion-controlled limiting current (Fig. 1c) was retained in CH_2Cl_2. There were important differences in i–E responses between those of $Ru_3(CO)_{12}$ and $Os_3(CO)_{12}$ and also when the counterion of the PPN salt was other than ClO_4^-.

First, with $Os_3(CO)_{12}$, the major effect of the PPN salt ($X = ClO_4^-$, OAc^-, Cl^-) was the elimination of the small oxidation waves seen on scan reversal in the cyclic voltammograms with TBAP supporting electrolyte (Fig. 2b). Further a new wave

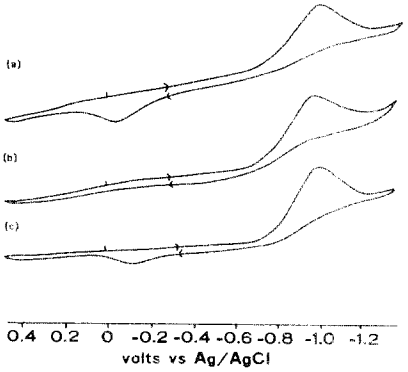

Fig. 3. Cyclic voltammograms of $Ru_3(CO)_{12}$ in CH_2Cl_2 under Ar. (a) $[Ru_3(CO)_{12}]$ 5×10^{-4} mol dm^{-3}, 293 K, 200 mV s^{-1}, Pt, 0.10 mol dm^{-3} [PPN][OAc]. (b) as for (a) except at 253 K. (c) $[Ru_3(CO)_{12}]$ 5×10^{-4} mol dm^{-3}, 293 K, 200 mV s^{-1}, Pt, [PPN][ClO_4]/[Bu_4N][OH], 0.10 mol dm^{-3} + 5×10^{-4} mol dm^{-3}.

appears on scan reversal at $E_{pa} \sim -1.13$ V irrespective of the gegenion: $i_{pa}/i_{pc} \sim 0.3$ at 200 mV s^{-1} at 293 K where i_{pc} refers to the primary reduction wave. The current for this oxidation wave does not change significantly with scan rate but increases at lower temperatures and it could represent the oxidation of *triangulo*-$Os_3(CO)_{12}^{2-}$.

A completely different picture emerged from the $Ru_3(CO)_{12}$ data. In this case the electrochemical behaviour is dependent on the gegenion X^-. When $X^- = OAc^-$, at 293 K, waves **B** and **C** (Fig. 1c) were lost to be replaced by a chemically irreversible oxidation wave at -0.06 V (Fig. 3a); the primary reduction current is smaller than when $X^- = ClO_4^-$ and $Ru_3(CO)_{12}$ is regenerated on repetitive scans. At temperatures below 253 K, or at 293 K under CO, the feature at -0.06 V disappears and the i–E responses are similar to those in Fig. 1c with the exception that **B** and **C** are absent (Fig. 3b). Electrochemistry of an authentic sample [10] of PPN^+ $[\mu\text{-}CH_3CO_2)Ru_3(CO)_{10}]^-$ showed that the feature -0.06 V is due to this anion. When the PPN^+OAc^- electrolyte solutions are left under Ar for $\sim$ 10 min, the primary reduction wave **A** disappears and the spectroscopic and electrochemical data show that $[(\mu\text{-}CH_3CO_2)Ru_3(CO)_{10}]^-$ is the only species in bulk solution.

Given that a coordinated CO group of a reduced Ru_3 species is apparently activated to nucleophilic attack close to the electrode surface we were intrigued by the possibility that traces of OH^- (or H_2O), invariably present in the sodium benzophenone ketyl preparations, were assisting the CO-labilization in electrode-induced or BPK catalysed $Ru_3(CO)_{12}$ substitution reactions [4]. Indeed when trace quantities of n-$Bu_4^+OH^-$ were added to $Ru_3(CO)_{12}$/[PPN][ClO_4]/CH_2Cl_2 solutions the primary reduction wave in the cyclic voltammograms remained unchanged but a small irreversible oxidation wave appeared at -0.1 V (Fig. 3c), close to that observed in the presence of OAc^-. We therefore assign this wave to the oxidation of *triangulo*-$[(\mu\text{-}C(O)OH)Ru_3(CO)_{10}]^-$.

$$Ru_3(CO)_{12}^{\cdot-} + OH^- \rightleftharpoons \overset{-e}{\longrightarrow} [(\mu\text{-}C(O)OH)Ru_3(CO)_{10}]^- + CO \qquad (3)$$

This feature disappears below 0 °C and under CO.

Erratic i–E responses were encountered when [PPN][Cl] was used as the electrolyte in the reduction of $Ru_3(CO)_{12}$. It was thought that this was due to the rapid homogeneous or heterogeneous reaction between [PPN][Cl] and $Ru_3(CO)_{12}$ described by Kaesz [9].

$$Ru_3(CO)_{12} + [PPN][Cl] \rightarrow [PPN][(\mu\text{-}Cl)Ru_3(CO)_{10}] + 2CO \quad (4)$$

By reference to the electrochemistry of an authentic sample of $[\mu\text{-}ClRu_3(CO)_{10}]^-$ this could be discounted on the electrochemical timescale. Features **B** and **C** in Fig. 1 were absent and there were no other oxidation peaks in the cyclic voltammograms on scan reversal after the primary two-electron reduction wave. The erratic feature in the cyclic voltammograms involving [PPN][Cl] was the appearance of a reduction wave at ~ -0.8 V on multiple scans. In some scans the primary reduction wave was lost completely whereas in others it still remained, albeit with lower i_{pc}. We have no explanation for this behaviour.

Controlled potential electrolyses in CH_2Cl_2

Controlled potential coulometry was carried out for the reduction of $M_3(CO)_{12}$ in CH_2Cl_2 in order to identify the species responsible for the various waves seen in the transient scans. Exhaustive reduction of $Ru_3(CO)_{12}$ or $Os_3(CO)_{12}$ at -1.0 or -1.3 V respectively at concentrations $> 5 \times 10^{-4}$ M, without rigorous exclusion of oxygen and water, gave the anions $M_3(CO)_{11}^{2-}$ and $M_6(CO)_{18}^{2-}$ in low yield with the passage of approximately one-electron per molecule of cluster. More informative data were obtained with solutions $< 5 \times 10^{-4}$ M and when precautions were taken to completely exclude oxygen and water; all the observations below refer to these conditions.

The reduction of $Ru_3(CO)_{12}$ in CH_2Cl_2/TBAP at a Pt basket electrode was carried out in a drybox until the current dropped to 5% of the initial value. At this point 1.9 ± 0.1 electrons per molecule of $Ru_3(CO)_{12}$ were consumed with the formation of dark red-brown air-sensitive solutions. A cyclic voltammogram of these solutions (Fig. 4) showed that the primary reduction wave of $Ru_3(CO)_{12}$ had virtually disappeared, as had features **B** and **C** in Fig. 1; feature **D** remained. The IR spectrum of these dilute solutions indicated that a new species other than

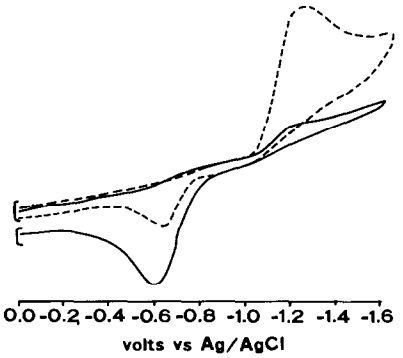

Fig. 4. Cyclic voltammograms of $Ru_3(CO)_{12}$ on Pt recorded before (------) and, after (———) controlled potential reduction at -1.1 V in CH_2Cl_2 in vacuo, in situ in an ESR cavity. $[Ru_3(CO)_{12}]$ 0.3×10^{-4} mol dm^{-3}. Scan rate 200 mV s^{-1}.

$Ru_3(CO)_{11}^{2-}$ or $Ru_6(CO)_{18}^{2-}$ was present but definitive IR data could not be obtained because of the low concentration and the IR spectrum of $Ru_3(CO)_{12}$ rapidly became dominant during FT-IR data collection [13].

Red solutions were also obtained from the reduction of $Os_3(CO)_{12}$ in CH_2Cl_2/TBAP at -1.3 V on the consumption of 1.8 ± 0.2 electrons per molecule of $Os_3(CO)_{12}$. The CV's showed the disappearance of the primary reduction wave of $Os_3(CO)_{12}$ and the chemically irreversible oxidation waves other than **D**. These reduced solutions were more stable than the Ru_3, especially if [PPN][ClO_4] was the supporting electrolyte, but again we have been unable to obtain reproducible IR data [13].

No paramagnetic species could be detected by ESR methods in the reduced solutions of $M_3(CO)_{12}$ in CH_2Cl_2 irrespective of whether the reduction was carried out external to, or in-situ in, the ESR cavity, or whether [TBAP] or [PPN] salts were supporting electrolytes. It was interesting that the high vacuum conditions attainable in this type of experiment gave cyclic voltammograms for reduced solutions of $Ru_3(CO)_{12}$ in which the current for feature **D** approached that for the primary reduction wave (cf. Fig. 4). This is consistent with an assignment of **D** to the oxidation of a diamagnetic species, $M_3(CO)_{12}^{2-}$.

Oxidation of the electrochemically reduced solutions of $Ru_3(CO)_{12}$ and $Os_3(CO)_{11}$ (CH_2Cl_2/TBAP) at the potential corresponding to wave **D** for the respective cluster regenerated neutral $M_3(CO)_{12}$ in recovered yields of between 60–80% with the consumption of 1.8 ± 0.1 electrons per molecule of initial cluster. Stabilization of the anionic species by [PPN] salts was shown by a 98% recovery of $Os_3(CO)_{12}$ from oxidation of reduced $Os_3(CO)_{12}/CH_2Cl_2$/[PPN][ClO_4] solutions with passage of 2.0 ± 0.1 electrons per molecule.

Solvent effects in the redox chemistry of $M_3(CO)_{12}$

DC polarograms and cyclic voltammograms of $Os_3(CO)_{12}$ in THF, acetone and CH_3CN show the same electrode processes described for CH_2Cl_2 as solvent with an appropriate shift in E_{pc} (Table 1).

Certain of the i–E responses for $Ru_3(CO)_{12}$ are dependent on the solvent.

(a) THF. DC polarograms indicated a diffusion-controlled, two-electron reduction wave. Distortion of the wave shape near the limiting current region was observed and, in this solvent, the current did not level off after the primary reduction wave but continued to increase at a diminished rate. All cyclic voltammograms exhibited a chemically irreversible reduction process (E_p -1.0 V, 200 mV s^{-1}) and a smaller oxidation process ($E_{pa} \sim -0.5$ V, 200 mV s^{-1}) which had the appearance of two merged peaks at scan rates > 1 V s^{-1}. No evidence of chemical reversibility of the reduction process was seen at scan rates up to 10^3 V s^{-1} and temperatures down to -70°C.

Controlled potential reduction of $Ru_3(CO)_{12}$ in TBAP/THF at -1.1 V under Ar gave an unstable red-brown solution with the consumption of ~ 1.8 electrons per molecule. $Ru_3(CO)_{11}^{2-}$ and $Ru_6(CO)_{18}^{2-}$ formed rapidly and relatively low yields ($< 10\%$) of regenerated $Ru_3(CO)_{12}$ were obtained on oxidation at ~ 0.1 V. The electrolyses of $Ru_3(CO)_{12}$ and $Os_3(CO)_{12}$ were also carried under vacuum in an ESR cavity but no paramagnetic species were detected in the temperature range 293–203 K.

The majority of electron-catalysed reactions of $Ru_3(CO)_{12}$ reported in the

literature [4] have been carried out in THF. In an endeavour to check for the formation of $Ru_3(CO)_{12}^{-\cdot}$ on the addition of Na^+ or K^+ benzophenone ketyl to $Ru_3(CO)_{12}$/THF solutions we carried out the addition of the reductant in-situ under vacuum, in an ESR cavity. An ESR signal (apart from ketyl) was not obtained at ambient temperatures but a paramagnetic species was observed if the solution was rapidly cooled to $-70°C$ after the addition of BPK. A spectrum at $g = 1.998$ (after subtraction of the ketyl spectrum) showed $^{99}Ru/^{101}Ru$ satellites appropriate to an Ru_3 species but simulation of the high-gain spectra suggested that more than one paramagnetic Ru_3 species was present [21]. These spectra were lost on rewarming to 0°C. Prior to the solution being cooled to $-70°C$ the cyclic voltammograms recorded simultaneously with the ESR spectra showed an increase in a broad wave corresponding to the features **B** and **D** in CH_2Cl_2. The observed ESR spectra are similar, but not identical to those reported by Watson [16] and Rieger and co-workers [5] from alkali metal reduction.

No paramagnetic species were detected in comparable reactions with $Os_3(CO)_{12}$ as substrate.

(b) Acetone. The *i–E* responses for $Ru_3(CO)_{12}$ in acetone have been described elsewhere [5] but essentially the results are similar to those in CH_2Cl_2 with the exception that feature **B** is more pronounced.

(c) CH_3CN. At scan rates less than 500 mV s^{-1} repetitive scans lead to a progressive negative shift in potential and smaller i_{pc} for the primary reduction wave of $Ru_3(CO)_{12}$ with eventual disappearance of the oxidation waves **B** and **C** (Fig. 1) on scan reversal. The slower the scan rate the more rapidly these changes occur. A small broad wave precedes the reduction peak on the initial scan; possibly a pre-wave denoting that a product is involved in a catalytic reaction. The ultimate reduction wave at $E_{pc} \sim -1.2$ V (500 mV s^{-1}) is assigned to the reduction of the derivative $Ru_3(CO)_{11}(NCCH_3)$ by reference to an authentic sample [17]. A progressive increase in CO concentration in solution causes a progressive shift of the reduction wave back to a potential corresponding the primary reduction wave of $Ru_3(CO)_{12}$. These data are consistent with an electron-catalysed reaction of $Ru_3(CO)_{12}^{-\cdot}$; that is, an $\vec{E}C\vec{E}$ reaction of the type

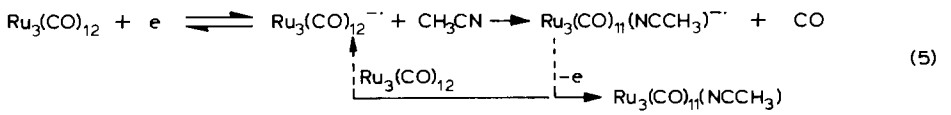

(5)

Controlled potential electrolysis of $Ru_3(CO)_{12}$ at -1.1 V in CH_3CN under Ar produces good yields ($\sim 60\%$) of the derivative $Ru_3(CO)_{11}(CH_3CN)$. However, the chain length of this reaction is extremely short (efficiency ~ 0.9 F mol^{-1}) although this is not surprising since ETC reactions involving CH_3CN are normally less efficient than those with nucleophiles like PR_3 [4]. In effect, the reaction with CH_3CN and $Ru_3(CO)_{12}$ is electron-induced rather than ETC with oxidation in bulk solution of the intermediate $[Ru_3(CO)_{11}(CH_3CN)]^{-\cdot}$ being heterogeneous (electrode) or via adventitious oxygen; this is consistent with the transient electrochemistry.

There was no evidence in the transient electrochemistry for an electron-induced reaction between $Os_3(CO)_{12}$ and MeCN to give $Os_3(CO)_{11}NCMe$ despite the stability of this adduct and its ease of preparation by thermal methods [18].

BPK-initiation also gives the $M_3(CO)_{11}(CH_3CN)$ derivatives but in the case of M = Os the yield is < 10%. It is doubtful whether this is a genuine electron-induced reaction.

Electrochemistry of $M_3(CO)_{12-n}(PPh_3)_n$

In order to look at the generality of the 2e primary reduction process and as a background to the catalysed reactions we investigated the electrochemistry of $M_3(CO)_{12-n}(PPh_3)_n$ complexes. DC polarographic and cyclic voltammetric data are given in Table 2.

In CH_2Cl_2, $Ru_3(CO)_{11}PPh_3$ exhibits a chemically irreversible primary reduction step 0.14 V more negative than $Ru_3(CO)_{12}$ and an irreversible oxidation step (Fig. 5). The DC polarographic limiting currents show that it is an overall two-electron reduction step. Particular features of the cyclic voltammogram of $Ru_3(CO)_{11}PPh_3$ are: (a) at slow scan rates (< 50 mV s^{-1}) there is a small wave at more negative potentials of the primary wave which can be assigned to the reduction of $Ru_3(CO)_{10}(PPh_3)_2$ (by comparison with the electrochemistry of an authentic sample [4]), this is presumably a result of an electron-induced reaction between $Ru_3(CO)_{11}PPh_3$ and PPh_3 from cluster decomposition (cf. eq. 5) or an endogenic bimolecular reaction.

$$2Ru_3(CO)_{11}PPh_3^{\cdot -} \rightarrow Ru_3(CO)_{12}^{\cdot -} + Ru_3(CO)_{10}(PPh_3)_2^{\cdot -} \quad (6)$$

TABLE 2

ELECTROCHEMICAL DATA FOR $M_3(CO)_{12-n}(PPh_3)_n$ (M = Ru, Os, $n = 1-3$) [a]

	DC Polarography [b]		Cyclic voltammetry [c]		
	Reduction		Reduction		Oxidation
	$E_{1/2}$ (V)	$E_{1/4} - E_{3/4}$ (mV)	E_{pc} (V)	E_{pa} (V)	E_{pa} (V)
M = Ru					
n = 1	−1.11	40	−1.24	−0.54	1.04
	−0.99	*55*	*−1.20*	*−0.53*	*1.27*
	(−0.98)	(50)	(−1.06)	(−0.40)	(1.07)
			(−1.20)		(1.27)
n = 2	−1.24	40	−1.31	−0.68	0.75, 0.87
				−0.50	1.13, 1.29
	−1.16	*55*	*−1.27*	*−0.47*	*1.07*
				−0.67	*1.40*
	(−1.18)	(50)	(−1.20)	(−0.47)	(0.86)
					(1.25)
n = 3	−1.49	50	−1.60	−0.64	0.63, 0.84
				−0.47	1.26
	−1.42	*60*	*−1.65*	*−0.51*	*0.73, 0.93*
	(−1.40)	(50)	(−1.49)	(−0.63)	(0.67, 0.87)
					(1.13)
M = Os					
n = 1	−1.54	80	−1.32	−0.41	
			−1.66	−0.10	

[a] At 293 K, volts vs. Ag/AgCl, normal type in CH_2Cl_2, italics in THF, brackets in acetone. Supporting electrolyte: CH_2Cl_2, TBAP; THF, TBAP, acetone, TEAP. [b] Drop time 0.5 s; scan rate 10 mV s^{-1}. [c] At Pt, scan rate 200 mV s^{-1}.

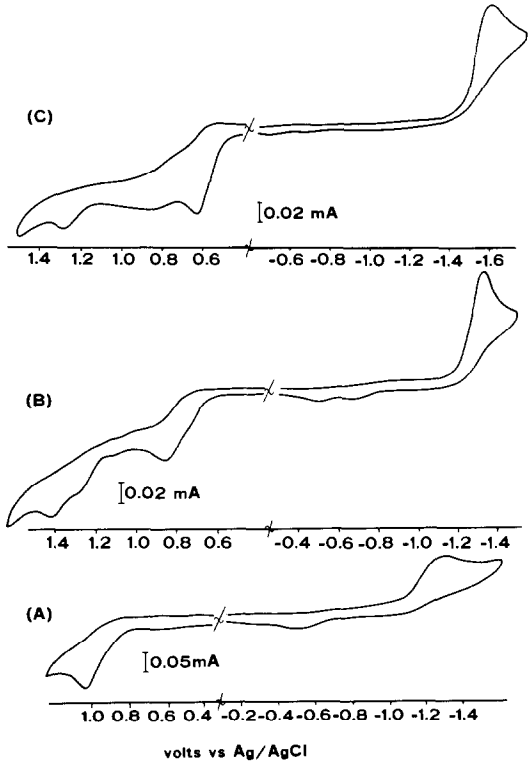

Fig. 5. Cyclic voltammograms in CH_2Cl_2 at Pt, 100 mV s^{-1}, 293 K under Ar, of (TBAP 0.1 mol dm^{-3}): (a) $Ru_3(CO)_{11}PPh_3$; (b) $Ru_3(CO)_{10}(PPh_3)_2$; (c) $Ru_3(CO)_9(PPh_3)_3$.

(b) the oxidation wave at $E_{pa} \sim -0.47$ V can be assigned to $Ru_3(CO)_{11}^{2-}$ (vide infra) which indicates that there is rapid Ph_3P dissociation from the $[Ru_3(CO)_{11}PPh_3]^{2-}$ species.

In acetone the overall electrochemical behaviour was similar to that in CH_2Cl_2 but the rates of reactions leading to $Ru_3(CO)_{10}(PPh_3)_2$ (and its radical anion) and $Ru_3(CO)_{12}$ were increased. Differences of this sort between acetone and CH_2Cl_2 have been noted in a number of cluster systems [1,3] and while the IR drop, with attendant problems of interpretation, is greater in CH_2Cl_2 the electrochemistry is usually cleaner. The i–E responses for $Ru_3(CO)_{11}PPh_3$ in THF were not well-behaved.

Data for the $Ru_3(CO)_{10}(PPh_3)_2$ and $Ru_3(CO)_9(PPh_3)_3$ are included in Table 2 and Fig. 5. The significant feature is the increasing chemical reversibility of the oxidation step and the absence of following ETC reactions (eq. 7) on the reduction scan.

$$Ru_3(CO)_{12-n}(PPh_3)_n^+ \underset{e}{\rightleftharpoons} Ru_3(CO)_{12-n}(PPh_3)_n \overset{e}{\rightleftharpoons}$$

$$Ru_3(CO)_{12-n}(PPh_3)_n^{-\cdot} \xrightarrow{\text{fast}} \text{products } (n = 2,3) \qquad (7)$$

A negative shift in E_{pc}^{red} and E_{pa}^{ox} as n increases is the expected trend.

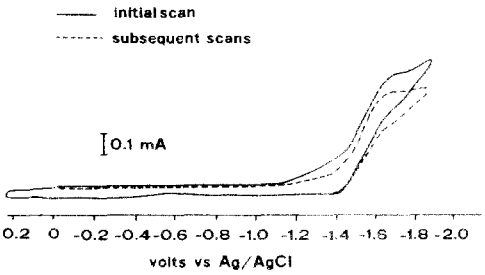

Fig. 6. Cyclic voltammogram of $Os_3(CO)_{11}PPh_3$ in CH_2Cl_2, 500 mV s^{-1}, at Pt, 293 K, TBAP 0.1 mol dm^{-3}

An overall two-electron reduction step is also observed for $Os_3(CO)_{11}PPh_3$ in CH_2Cl_2 but in contrast to $Ru_3(CO)_{11}PPh_3$ there is no evidence for the formation of $Os_3(CO)_{10}(PPh_3)_2$ by an ECE reaction. The surprising feature is the partial chemical reversibility of the primary reduction wave at 20°C (Fig. 6) and its chemical reversibility at low temperatures; the oxidation process does not occur within the solvent limit.

$$Os_3(CO)_{11}PPh_3 + 2e \rightleftharpoons Os_3(CO)_{11}PPh_3^{2-} \quad (8)$$

Unfortunately the $Os_3(CO)_{12-n}(PPh_3)_n$ ($n = 2$, 3) complexes were not reduced within the solvent limit so that the generality of reductive reversibility could not be tested; studies on other Lewis base derivatives are in hand.

Electron-catalysed substitution of $M_3(CO)_{12}$

Cyclic voltammograms for the reduction of $Ru_3(CO)_{12}$ in the presence of a three molar excess of PPh_3 are shown in Fig. 7 for CH_2Cl_2, acetone and THF. A quantitative interpretation of the new reduction waves is difficult due to the small difference in peak potentials of the derivatives $Ru_3(CO)_{12-n}(PPh_3)_n$ (Table 2). In CH_2Cl_2 there is a wave due to the reduction of $Ru_3(CO)_{11}PPh_3$, in THF both $Ru_3(CO)_{11}PPh_3$ and $Ru_3(CO)_{10}(PPh_3)_2$ can be recognised, whereas substitution is less specific in acetone with all three derivatives $Ru_3(CO)_{12-n}(PPh_3)_n$ ($n = 1$–3) being produced. Since the peak currents are small for the reduction waves associated with these complexes, even at scan rates of ~ 50 mV s^{-1}, the $\vec{E}C\vec{E}$ reaction must be slow. This is consistent with the short lifetime of *triangulo*-$Ru_3(CO)_{12}^{-\cdot}$.

Cyclic voltammograms of $Os_3(CO)_{12}$ in CH_2Cl_2 or THF at scan rates 50–500 mV s^{-1} were unchanged by the addition of up to a 20 molar excess of PPh_3 (or $P(OPh)_3$).

Solvent effects were important in the bulk cathode-induced substitution reactions of $Ru_3(CO)_{12}$ in the presence of equimolar amounts of PPh_3. In CH_2Cl_2 a slow decay of the electrolysis current to ~ 10% of the initial value gave a ~ 70% yield of $Ru_3(CO)_{11}PPh_3$ with an efficiency of ~ 0.5 F mol^{-1}. In acetone the electron-induced reaction was non-specific and the decay in current was accompanied by the formation of all derivatives $Ru_3(CO)_{12-n}(PPh_3)_n$ ($n = 1$–3). Significantly, in THF the small electrolysis current decayed slightly with concomitant rapid darkening of the solution colour. After 3 min analysis showed complete conversion to Ru_3-

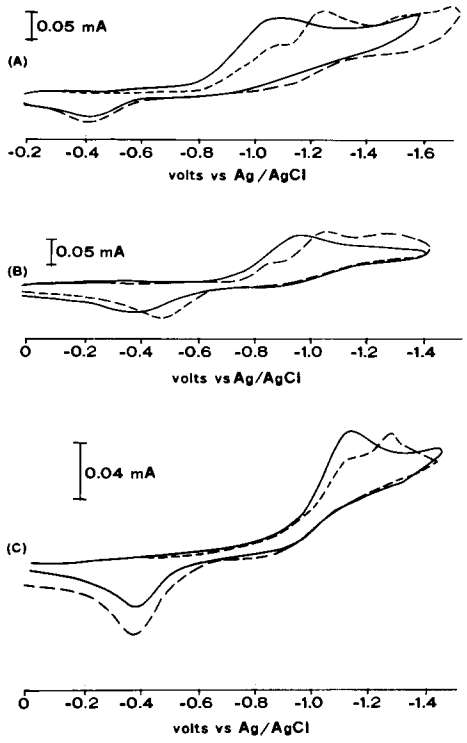

Fig. 7. Cyclic voltammograms of 0.5 mM $Ru_3(CO)_{12}$ in CH_2Cl_2, 200 mV s^{-1}, at Pt, in the absence (———) and presence (------) of 1.5 m*M* PPh_3. (a) acetone; (b) THF; (c) CH_2Cl_2.

$(CO)_{11}PPh_3$ with a consumption of charge corresponding to $\sim 1.2 \times 10^{-4}$ electrons per molecule of $Ru_3(CO)_{12}$. Reduction of $Os_3(CO)_{12}$ in CH_2Cl_2 in the presence of equimolar PPh_3 gave a 35% yield of $Os_3(CO)_{11}PPh_3$ with an efficiency of ~ 0.9 F mol^{-1}.

Electrochemistry of $[HRu_3(CO)_{11}]^-$, $[Ru_3(CO)_{11}]^{2-}$, $[Os_3(CO)_{11}]^{2-}$ *and* $[Ru_6(CO)_{18}]^{2-}$

Shore and co-workers [19] have isolated a number of anionic clusters from the chemical reduction of $Ru_3(CO)_{12}$. Several were considered as species responsible for the oxidation waves in the cyclic voltammograms and accordingly their electrochemistry was investigated in CH_2Cl_2 (as [PPN] or Bu_4N^+ salts). Complex *i–E* responses were obtained for Ru_4 clusters but as it was clear that they are not participating in the electrode processes for $Ru_3(CO)_{12}$ these will not be considered here.

Our results for $Ru_3(CO)_{11}^{2-}$ were substantially as reported by Rieger and co-workers [5] and $Os_3(CO)_{11}^{2-}$ behaves similarly being oxidised at more positive potentials. Wave **B**, Figs. 1, 2, is assigned to the oxidation of these anions.

Gieger and Tulyathan [20] have shown that the reduction of $Os_6(CO)_{18}$ proceeds by an overall two-electron, chemically reversible, process measured by us at $E_{1/2}$ ~

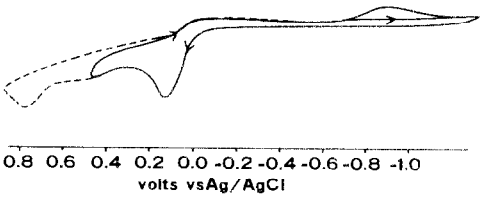

Fig. 8. Cyclic voltammogram of [PPN][$HRu_3(CO)_{11}$] in CH_2Cl_2 on Pt, in CH_2Cl_2 at 293 K; 200 mV s^{-1}.

−0.17 V vs. Ag/AgCl. This electron-transfer process incorporates an octahedron-bicapped/tetrahedron structural rearrangement [21]. In contrast, we find that the oxidation of octahedral $Ru_6(CO)_{18}^{2-}$ is an overall two-electron process but chemically irreversible under 'normal' conditions; E_{pa} −0.35 V vs. Ag/AgCl at 200 mV s^{-1}. However, this process becomes chemically reversible in dilute CH_2Cl_2 solutions at 293 K providing water and oxygen are totally removed from the system. Even so, the half-life of the "$Ru_6(CO)_{18}$" on the electrochemical timescale is less than 10^{-3} s and it is unlikely that it could be isolated. A simultaneous 2-electron transfer is unlikely but oxidation of $Ru_6(CO)_{18}^{2-}$ in CH_2Cl_2 in-situ in the ESR cavity at low temperatures did not generate any detectable paramagnetic species.

The hydrido-anion, $HRu_3(CO)_{11}^-$, undergoes a chemically irreversible but diffusion controlled oxidation at E_{pa} 0.12 V in CH_2Cl_2 on Pt, and a further irreversible oxidation at 0.78 V (Fig. 8). The first oxidation process becomes more reversible as the temperature is decreased and at fast scan rates (> 500 mV s^{-1}) but the reversibility is unaffected by CO. No reduction steps are observed on the initial

$$HRu_3(CO)_{11}^- \rightleftharpoons HRu_3(CO)_{11}^{\cdot} + e \qquad (10)$$

scan but on scan reversal a wave appears at −0.98 V corresponding to the reduction of $Ru_3(CO)_{12}$; i_{pc} for this process increased under CO. Consequently, the formation of $Ru_3(CO)_{12}$ can be attributed to equilibrium (11) similar to that proposed by Shore [22] for $HRu_3(CO)_{11}^-$ but involving $HRu_3(CO)_{11}^{\cdot}$.
Decomposition of the unstable $HRu_3(CO)_{11}^{\cdot}$ would provide the CO and $Ru_3(CO)_{12}^{\cdot-}$ will be oxidised at potentials > −0.9 V. $HRu_3(CO)_{11}^-$ is regenerated after the $\vec{E}\vec{C}\vec{E}$ reduction step of $Ru_3(CO)_{12}$ indicating that the equilibrium (11) is also rapid in the reverse direction (note that wave **B** in Fig. 1 is not observed in Fig. 8).

Discussion

Redox processes for $M_3(CO)_{(12-n)}(PPh_3)_n$ ($n = 0$–3)

(a) Primary electrode processes. This study has established that the *triangulo* clusters $M_3(CO)_{12}$ (M = Ru, Os) and $Ru_3(CO)_{12-n}(PPh_3)_n$ ($n = 1$–3) and $Os_3(CO)_{11}PPh_3$ all participate in a primary diffusion-controlled two-electron reduction process at the electrode surface.

The following mechanistic schemes for the reduction step were investigated using digital simulation [22] and convolution techniques [23].

(a) ECE

$$M_3(CO)_{12} + e \overset{k_{s1}}{\rightleftharpoons} M_3(CO)_{12}^{-\cdot}$$

$$M_3(CO)_{12}^{-} \overset{k}{\rightarrow} M_3(CO)_{12}^{-\cdot\star}$$

$$M_3(CO)_{12}^{-\star} + e \overset{k_{s2}}{\rightleftharpoons} M_3(CO)_{12}^{2-\star}$$

(b) EE

$$M_3(CO)_{12} + e \overset{k_{s1}}{\rightleftharpoons} M_3(CO)_{12}^{-\cdot}$$

$$M_3(Co)_{12}^{-\cdot} + e \overset{k_{s2}}{\rightleftharpoons} M_3(CO)_{12}^{2-}$$

(c) Simultaneous 2 − e

$$M_3(CO)_{12} + 2e \overset{k_{s1}}{\rightleftharpoons} M_3(CO)_{12}^{2-}$$

(d) Disproportionation

$$M_3(CO)_{12} + e \overset{k_{s1}}{\rightleftharpoons} M_3(CO)_{12}^{-\cdot}$$

$$2M_3(CO)_{12}^{-\cdot} \overset{k}{\rightarrow} M_3(CO)_{12}^{2-} + M_3(CO)_{12}$$

SCHEME 1

Mechanism (c) did not give an accurate digital simulation of the experimental cyclic voltammograms whereas (a), (b) and (d) allowed accurate simulation when the homogeneous rate constants were sufficiently large and not rate-controlling. The best match of theoretical and experimental cyclic voltammograms was obtained with values of $k_s = 2 \times 10^{-3}$ cm s^{-1} and $\alpha = 0.37$[23] (the characteristics of the cyclic voltammogram depend primarily on the first charge transfer) and $k > 15$ s^{-1} (mechanism (a)) and $> 6 \times 10^7$ M^{-1} s^{-1} (mechanism (d)). Analysis of changes in the convoluted current with scan rate and potential indicated that mechanism (a), the $\vec{E}\vec{C}\vec{E}$ mechanism, was the most reasonable explanation for the overall two-electron step.

The chemical irreversibility of the reduction step up to 10^4 V s^{-1} shows that the half-life of the *triangulo*-$M_3(CO)_{12}^{-\cdot}$ is less than 10^{-6} s in CH_2Cl_2 at 293 K [24].

Rieger and co-workers [5] have speculated that the resultant species of the very fast chemical reaction is the "open" or linear $M_3(CO)_{12}$.

$$M_3(CO)_{12} + e \rightleftharpoons M_3(CO)_{12}^{-\cdot} \rightarrow {}^{\star}M_3(CO)_{12}^{-\cdot} \overset{e}{\rightleftharpoons} {}^{\star}M_3(CO)_{12}^{2-} \qquad (11)$$

This certainly accounts for the high recovery yields of $M_3(CO)_{12}$ in coulometric

experiments, as well as at the electrode, and is consistent with the addition of an electron to an antibonding (M_3-based) LUMO. Further, the resultant opened $M_3(CO)_{12}^{2-\bullet}$ species will be diamagnetic as required by our ESR data. Attempts to isolate the products of the ECE reactions were thwarted by the sensitivity of the species towards water and the concentration dependence of the electrochemical behaviour. At low substrate concentrations and under dry box or high vacuum conditions or at high scan rates only one oxidation wave (**D**) is seen. This is assigned to the oxidation of the opened $M_3(CO)_{12}^{2-}$.

$$M_3(CO)_{12}^{2-} \overset{(D)}{\underset{-e}{\rightleftharpoons}} M_3(CO)_{12}^{-\bullet} \rightleftharpoons M_3(CO)_{12} \tag{12}$$

The irreversibility of this process shows that the opened radical anion $M_3(CO)_{12}^{-\bullet}$ also has a short lifetime ($t_{1/2} < 10^{-6}$ s in CH_2Cl_2).

Once the concentration is increased or traces of water are present CO-dissociative and bimolecular cluster reactions occur the products of which dominate the oxidation scan.

$$M_3(CO)_{12}^{2-\bullet} \rightarrow M_3(CO)_{11}^{2-\bullet} + CO \tag{13}$$

$$M_3(CO)_{11}^{2-} \overset{(B)}{\rightleftharpoons} M_3(CO)_{11}^{-\bullet} + e$$

$$M_3(CO)_{11}^{2-} + M_3(CO)_{12} \rightarrow M_6(CO)_{18}^{2-} + 5CO \tag{14}$$

We suggest that the major route to $M_3(CO)_{11}^{2-}$ is via nucleophilic attack by H_2O on $M_3(CO)_{12}^{2-}$ rather than (13). Note that wave (**B**) is absent in vacuo conditions which would encourage (13).

$$M_3(CO)_{12}^{2-} + H_2O \rightleftharpoons \left\{M_3(CO)_{11}\left[\eta^1\text{-}C(O)\text{-}OH_2\right]\right\}^{-} \rightarrow M_3(CO)_{11}^{2-} + CO + H_2O \tag{15}$$

So, the ultimate products from controlled potential electrolysis of $M_3(CO)_{12}$ in CH_2Cl_2 are $M_6(CO)_{18}^{2-}$ and $M_3(CO)_{11}^{2-}$. A linear $Ru_3(CO)_{12}^{2-}$ species has been postulated [14] as a product of the K/Hg reduction of $Ru_3(CO)_{12}$ but there was no indication of a species with a comparable $\nu(CO)$ spectrum in the products of controlled potential electrolysis. Wrighton and co-workers also speculated that an opened $Ru_3(CO)_{12}$ cluster was involved in photochemical substitution reactions [25]. $Os_3(CO)_{12}X_2$ [26] and $Os_3(CO)_{12}R_2$ [27] (R = Me, H) are well-established opened trinuclear osmium complexes. Opened triangular M_3 cores are found in $Os_3(CO)_{12}[MeOC(O)N)_2]$ [28] and $Ru_3(CO)_{10}(NO)_2$ [29] but both complexes utilize a bridging group to stabilise the opened structure. Given the fast rates of conversion between reduced *triangulo* and opened reduced $M_3(CO)_{12}$ species it is conceivable that $M_3(CO)_{12}^{2-}$ has a triangular structure but with an opened M–M bond supported by bridging carbonyl groups.

Because of the short lifetimes of $M_3(CO)_{12}^{-\bullet}$ it is not possible to give a quantitative estimate of the relative rates of *trangulo*-opened interconversion between Ru_3 and Os_3. Nonetheless, the lack of electron-initiated nucleophilic substitution reactions with $Os_3(CO)_{12}$ (vide infra) and greater dominance of wave **D** in the Os_3 scans under 'normal' conditions strongly indicates that the conversion and

reduction to opened $Os_3(CO)_{12}^{2-}$ is faster than the comparable Ru_3 conversion. This would be consistent with the greater stability of known opened Os_3 structures. There is an interesting correlation between the differences in electrochemical behaviour of $Ru_3(CO)_{12}$ and $Os_3(CO)_{12}$ and their photochemistry [25]. Ru–Ru bond breaking dominates the photobehaviour of $Ru_3(CO)_{12}$ whereas fragmentation of the Os_3 unit occurs only after substitution by a Lewis base at each Os atom. While the two activation processes are not strictly comparable (i.e. electron addition to a LUMO compared with photoexcitation) the different character of the LUMO or excited state in the two complexes is undoubtedly important.

(b) Effect of [PPN] salts. New electroactive species appear on scan reversal after the reduction of $Ru_3(CO)_{12}$, but not $Os_3(CO)_{12}$, in the presence of [PPN][X] $X = OAc^-$, OH^-, Cl^-. This correlates with the specific catalytic reaction by [PPN] salts delineated by Kaesz and co-workers [9] and one could look for a common explanation. Since the diffusion current for the production of $Ru_3(CO)_{12}$ is less than two electrons per molecule, our interpretation is that attack by the nucleophile on *triangulo* or opened $Ru_3(CO)_{12}^{-\cdot}$ is very fast giving a species which is not oxidised in the potential range. At ambient temperature a further slow chemical step occurs to give the species $[Ru_3(\mu\text{-Nu})(CO)_{10}]^-$. We suggest the intermediate species are those detected by Kaesz [9] and Ford [10], $[Ru_3(\eta^1\text{-C(O)(-Nu)}(CO)_{11}]^-$, the result of nucleophilic attack on a coordinated CO group of $Ru_3(CO)_{12}^{-\cdot}$ or $Ru_3(CO)_{12}^{2-}$.

$$Ru_3(CO)_{12}^{-\cdot} + :Nu \underset{-e}{\overset{\text{fast}}{\rightleftharpoons}} \left[Ru_3(\eta^1\text{-C(O)(-Nu)}(CO)_{11})\right]^- \tag{16}$$

$$\left[Ru_3(\eta^1\text{-C(O)(-Nu)}(CO)_{11}\right]^- \xrightarrow{\text{slow}} \left[Ru_3(\mu\text{-Nu})(CO)_{10}\right]^- + 2CO \tag{17}$$

At low temperatures or under CO reaction (17) is electrochemically insignificant (except when $X = Cl^-$) but even so, the oxidation waves associated with the "normal" *i–E* response for $Ru_3(CO)_{12}$ (i.e. **B** and **D**) are also absent. Reaction 16 is therefore still operative under these conditions and, given the half-life of only $< 10^{-6}$ s for $Ru_3(CO)_{12}^{-\cdot}$, it suggests that nucleophilic attack could involve the opened species. The ramifications for [PPN]-catalysed reactions in the absence of an electrode are that these may also involve bond-opening.

The diffusion current for the reduction of $Os_3(CO)_{12}$ in the presence of [PPN] salts remains at two electrons per molecule indicating that the corresponding reaction 16 for *triangulo*-$Os_3(CO)_{12}^{-\cdot}$ is too slow to compete with the $\vec{E}C\vec{E}$ step (eq. 11). This fits into the general picture of restricted catalytic substitution with $Os_3(CO)_{12}$ (vide infra).

(c) Solvent effects. The $\vec{E}C\vec{E}$ step (eq. 11) occurs in all solvents, the principal differences in *i–E* response arising from different rates for CO-dissociation (faster in polar solvents) and nucleophilic substitution (with CH_3CN). Furthermore, it is difficult to exclude water from acetone solutions. THF poses problems because of irreproducibility of the cathodic profile of the CV scans but under normal conditions the current due to the oxidation of $M_3(CO)_{11}^{2-}$ is smaller than in acetone or CH_2Cl_2. Two factors could account for this. First, the THF would be very dry; second, THF does appear to have the facility for stabilising radical anions and the rate of $M_3(CO)_{12}^{2-}$ formation – the precursor to $M_3(CO)_{11}^{2-}$ if eq. 15 is correct –

could be lower. These observations are compatible with the more efficient nucleophilic substitution in this solvent.

Catalytic substitution of $Ru_3(CO)_{12}$ and $Os_3(CO)_{12}$

Rapid nucleophilic substitution of $Ru_3(CO)_{12}$ can be initiated by three methods: (1) a [PPN] salt [9], (2) a chemical reductant such as BPK [4], (3) an electrode. In contrast, activation of $Os_3(CO)_{12}$ towards substitution is slow and with most nucleophiles thermal substitution is of comparable efficiency.

Observations which have a bearing on the mechanism of activated substitution are:

(a) comparable rates and specificity of substitution are obtained with methods (1) and (2) in CH_2Cl_2 whereas reactions via (3) are as specific but slower in similar solvents.

(b) initiated reactions (2) and (3) are only specific and rapid in THF (electrode-initiated reactions are relatively specific in CH_2Cl_2 but this is due to the slow rate of nucleophilic substitution); electrochemically-generated Ru_3 paramagnetic anions were only detected in THF at low temperatures.

(c) the rate of [PPN]-initiated substitution is not affected by solvent except that catalysis was prevented by strong hydrogen-bonding solvents; further, Kaesz and co-workers [9] noted that a trace of moisture was required for catalysis using [PPN][Cl].

(d) there is evidence that reactions of type (1) proceed via gegenion attack on a coordinated carbonyl group.

(e) even at relatively high concentrations of Ph_3P (> 20 mole excess) the $\vec{E}C\vec{E}$ step to produce $Ru_3(CO)_{11}PPh_3$ cannot compete effectively with the $\vec{E}C\vec{E}$ step: that is, Ru–Ru bond cleavage is as fast as nucleophilic substitution which traps the triangulo $Ru_3(CO)_{12}^{\cdot-}$.

A rationale for these observations can be found in the influence of the solvent, the differing timescales of reactions and the possible reaction pathways for the activated Ru_3 species. THF is known to facilitate electron transfer catalysed reactions in other systems [1] and this can be attributed to solvation and ion-pair (particularly with Na^+) stabilization of the reactive radical anions [12]. Bulk chemical reduction will also generate a much higher concentration than electrochemical initiation. Furthermore, nucleophilic attack by OH^- on a coordinated CO group was indicated by the electrochemical data and this may well contribute to the overall activation in THF/BPK reactions as traces of OH^- will inevitably be present in the BPK reactions unless special precautions are taken.

Despite the fact that there is no evidence for "stable" *triangulo* or opened $Ru_3(CO)_{12}^{\cdot-}$ (i.e. chemical reversibility) on the electrochemical timescale, it does not preclude "stability" away from the electrode or under homogeneous reactivity involving BPK. Under electrochemical conditions the half-life of *triangulo* $Ru_3(CO)_{12}^{\cdot-}$ is $< 10^{-6}$ s and so opened $Ru_3(CO)_{12}^{\cdot-}$ is being formed essentially at the electrode surface. Since its reduction is thermodynamically favoured it is immediately reduced to the substitution-inert dianion. The net result of the equilibrium (12) is that *triangulo* $Ru_3(CO)_{12}^{\cdot-}$ is converted to opened $Ru_3(CO)_{12}^{2-}$.

Further, homogeneous electron transfer (eq. 18) at or near the electrode surface will also decrease the concentration of reactive radical anions.

(18)

With chemical initiation in dilute solutions the radical anions will not necessarily be reduced nor will eq. 18 occur before attack by the nucleophile takes place. Once nucleophilic substitution has occurred the ETC cycle (eq. 19) is initiated but, even under the optimum conditions, chain-termination steps clearly reduce the efficiency of the cycle unless THF is the solvent.

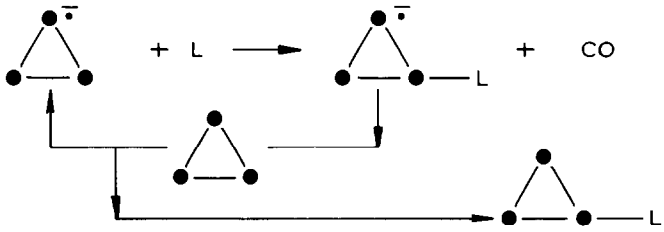

(19)

Moreover, the rate of homogeneous electron transfer after the first substitution step is only fast enough in THF to outrun the further substitution processes which give $Ru_3(CO)_{10}(PPh_3)_2$ and $Ru_3(CO)_9(PPh_3)_3$. Note that the rate of thermal substitution increases with the degree of substitution [30].

The relationship between [PPN] salt-activated and electron-activated substitution is a matter for conjecture but it is possible that [PPN]-assisted nucleophilic attack at a CO group also incorporates rupture of a Ru–Ru bond. [PPN] would stabilize any anionic intermediates. Metal–metal bond rupture under mild conditions has been demonstrated for metal clusters [31], especially for the Ru_3 moiety, and the trend of facile Fe–Fe rupture/fragmentation, Ru–Ru rupture/no fragmentation, no Os–Os rupture follows the expected trend in thermodynamic metal–metal bond strength.

Conclusion

This study has confirmed the generality of an overall two-electron $\vec{E}C\vec{E}$ process for $M_3(CO)_{12}$ (M = Ru, Os) and $M_3(CO)_{12-n}(PPh_3)_n$ in all solvents which probably involves a metal–metal bond cleavage step. Concomitant with reduction of the $M_3(CO)_x$ unit one finds solvent-dependent, CO-dissociative and ligand dissociative pathways as well as nucleophilic-attack on a coordinated CO group.

Trends in the redox behaviour of the $M_3(CO)_{12}$ (M = Fe, Ru, Os) clusters can be rationalized in both the thermodynamic and kinetic sense. Scheme 2 summarises the pathways open to the initially formed $M_3(CO)_{12}^{-\cdot}$ radical anion (*-represent an 'opened' structure).

Step A, conproportionation, is only important for $Fe_3(CO)_{12}$ and it is only with this cluster that the $M_3(CO)_{12}^{-\cdot}$ species has been characterised [2,25]. The thermodynamic driving force for conproportionation is probably the instability of a *triangulo*-$Fe_3(CO)_{12}^{2-}$ complex. Pathway B, decreases in importance from Fe → Os which may be due to steric factors; the solvent effects on this pathway are expected. The increasing thermodynamic strength of the metal–metal bond down a group are reflected in the absence of pathway E in other than M = Fe and the increasing rate of pathway C from Fe → Os.

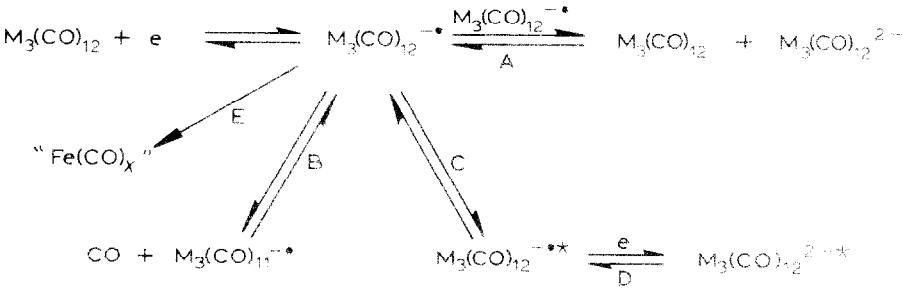

SCHEME 2

The work described herein was stimulated by an apparent conflict of experiment and theory. Reports of irreversible electrode processes but efficient ETC-catalysed reactions for $Ru_3(CO)_{12}$ contradicted the general view that suitable substrates are those that exhibit chemically reversible redox behaviour. It is clear from this study that the important criteria are relative, rather than absolute, rates of nucleophilic substitution and alternative pathways involving the key radical anions. ETC-catalysed reactions with $Fe_3(CO)_{12}$ are fast and efficient because of the high $M_3(CO)_{12}^{-\bullet}$ concentration through pathway A, the low yields are due to fragmentation reactions (E). Pathway C reduces the available $M_3(CO)_{12}^{-\bullet}$ (M = Ru, Os) with consequential lower ETC efficiency. Selective and apparently fast nucleophilic substitution with $Ru_3(CO)_{12}$ via BPK initiation is, we believe, due to the intermediacy of $[\eta^1\text{-}C(O)(X)Ru_3(CO)_{11}]^-$ species as well as an ETC-catalysed reaction. Finally, the electrochemical behaviour in the presence of active [PPN] salts parallels that found for [PPN]-catalysed nucleophilic substitution in solution, in particular the inactivity of $Os_3(CO)_{12}$. It is conceivable that Ru–Ru bond cleavage has a role in the [PPN]-catalysed reactions.

These trends in the electrochemical mechanisms correlate well with those attendant upon photochemical initiation.

Experimental

$Ru_3(CO)_{12}$ and $Os_3(CO)_{12}$ were used as received if TLC and IR analysis indicated a satisfactory purity; otherwise they were crystallized from CH_2Cl_2/hexane. The derivatives $M_3(CO)_{12-n}(PPh_3)_n$ were prepared by literature methods [4]. $[PPN^+][X^-]$ salts were prepared by the literature procedure [32,33] but for the electrochemical work it was necessary to recrystallize the salts many times and dry in vacuo in order to obtain a satisfactory electrolyte. TBAP (tetrabutylammonium perchlorate) (Fluka) was recrystallized from EtOAc and dried in vacuo at 353 K; TEAP (tetraethylammonium perchlorate) (Fluka) was recrystallized from methanol and dried in vacuo at 343 K. BPK was obtained from a THF purification still. The cluster anions $Ru_3(CO)_{11}^{2-}$, $Ru_6(CO)_{18}^{2-}$, $Ru_4(CO)_{13}^{2-}$, $Os_3(CO)_{11}^{2-}$, $Os_6(CO)_{18}^{2-}$ and $HRu_3(CO)_{11}^-$ were prepared by literature procedures [19,34] as their PPN^+ or $^nBu_4N^+$ salts and characterised by IR and chemical analysis. The solvents were purified according to the methods described elsewhere [1]. Polarographic and voltammeric measurements were made with one of the following sets of instrumentation: a PAR 174 analyser and a PAR 175 universal programmer connected to an

X-Y recorder or Tectronix storage oscilloscope or an interfaced Apple//e microcomputer (20 mV s^{-1}): a Hi-Tek Instruments waveform generator with the current amplified and fed directly into a Gould storage oscilloscope and replotted on a X-Y recorder.

A standard 3-electrode cell was designed to allow the tip of the reference electrode to approach within 2 mm of the working electrode and used for measurements with scan rates up to 50 V s^{-1} or in the dry-box. For fast scan measurements (50–15000 V s^{-1}) a two-electrode cell configuration was used. The electrodes can show a variable response if not freshly cleaned and polished. The microelectrode was a 10 μm diameter Pt disc made by sealing 10 μm wire into glass and polishing the surface with alumina powder. All measurements were carried out under Ar with the electrolyte, either under normal laboratory conditions or in a dry-box, and cluster concentrations given in the Tables and Figures. Controlled potential electrolyses and coulometric determinations were carried out in an oxygen-free Ar atmosphere box or in a system where the whole apparatus was enclosed in a large plastic bag filled under a positive pressure of oxygen-free argon. Infra-red cells were filled in an oxygen-free environment using gas-tight syringes. The standard cell for bulk electrochemical work has been described previously [1]. All experiments were done at least in duplicate. ESR spectra were recorded on a Varian E-4 X-band ESR spectrometer using a specially-built 3-electrode electrochemical cell for in-situ measurements which enabled the electrolysing potential to be accurately controlled and provided concurrent cyclic voltammograms [35]. Procedures for carrying out measurements on solutions involving a chemical reductant, or those under vacuum, have been given elsewhere [36]. Electrolyses were carried out ~ 0.2 V negative of the primary reduction wave.

Potential data (vs. Ag/AgCl) were referenced against the ferrocene$^{+/0}$ couple in a particular solvent using the values given earlier [36]. The peak-to-peak separation for the ferrocene couple (usually 60 mV if the electrodes were carefully positioned) was taken as the diffusion-controlled parameter. Diffusion coefficients, the influence of resistance effects and heterogeneous rate constants were obtained from digital simulation of the cyclic voltammograms using programs based on the relevant statements given by Feldberg [22], these were run on a Digital Vax 11/780 computer. Background currents were simulated as linear potential ramps. Convolution analytical programs were based on the algorithm given by Bard and Faulkner [23]. The number of electrons transferred in a particular redox process was determined by comparison [1] with the one-electron ferrocene$^{+/0}$, $Fe_3(CO)_{12}{}^{0/-}$ or $PhCCo_3(CO)_9{}^{0/-}$ couples as well as through the usual diagnostic electrochemical parameters.

Acknowledgements

We thank Professors Bruce and Stone for the preparation of $Ru_3(CO)_{12}$ and $Os_3(CO)_{12}$ respectively, Mr. S.R. Forsyth and Mr. D. Luscombe for technical assistance and Professor H. Kaesz, Professor, P. Ford and Professor W.E. Geiger for unpublished data.

References

1 A.J. Downard, B.H. Robinson and J. Simpson, Organometallics, 5 (1986) 1140.
2 P.A. Dawson, B.M. Peake, B.H. Robinson and J. Simpson, Inorg. Chem., 19 (1980) 465.

3 M. Arewgoda, B.H. Robinson and J. Simpson, J. Am. Chem. Soc., 105 (1983) 1893; M.I. Bruce, P.C. Kehoe, J.G. Matisons, B.K. Nicholson, P.H. Rieger, and M.L. Williams, J. Chem. Soc., Chem. Commun., (1982) 442.
4 M.I. Bruce, J.G. Matisons and B.K. Nicholson, J. Organomet. Chem., 247 (1983) 321.
5 J.E. Cyr, J.A. De Gray, D.K. Gosser, E.S. Lee and P.H. Rieger, Organometallics, 4 (1985) 950.
6 A. Downard, B.H. Robinson and J. Simpson, Int. Chem. Congress, Pacific Basin Soc. Honolulu, 1984, Abstract 07N04.
7 D. Miholova, J. Fiedler and A.A. Vlcek, J. Electroanal. Chem., Interfacial Electrochem., 143 (1983) 195.
8 We follow the wave designation used by Rieger and coworkers [5].
9 G. Lavigne and H.D. Kaesz, J. Am. Chem. Soc., 106 (1984) 4647.
10 M. Anstock, D. Taube, D.C. Cross and P.C. Ford, J. Am. Chem. Soc., 106 (1984) 3969 [11].
11 D.J. Darensbourg, M. Pala and J. Waller, Organometallics, 2 (1983) 1285.
12 C.M. Kirk, B.M. Peake, B.H. Robinson and J. Simpson, Aust. J. Chem., 36 (1983) 441.
13 From the data with $[PPN]ClO_4$ as electrolyte ν(CO) bands at 2062m, 2032s, 2001s, 1961s, (M = Ru), 2058m, 2019s, 1992s, 1952s cm^{-1} (M = Os) could be assigned to the 'opened' $M_3(CO)_{12}^{2-}$.
14 G.B. McVicker and M.A. Vannice, J. Catalysis, 63 (1980) 25.
15 A.J. Downard, Ph.D. Thesis, University of Otago, 1984.
16 B.M. Peake, B.H. Robinson, J. Simpson and D. Watson, J. Chem. Soc., Chem. Commun., (1974) 945.
17 G.A. Foulds, B.F.G. Johnson and J. Lewis, J. Organomet. Chem., 296 (1985) 147.
18 B.F.G. Johnson, J. Lewis and D. Pippard, J. Organomet. Chem., 213 (1981) 249.
19 A.A. Bhattacharyya and S.G. Shore, Organometallics, 2 (1983), 1251; A.A. Bhattacharyya, C.C. Nagel and S.G. Shore, ibid., 2 (1983) 1187.
20 W.E. Geiger and B. Tulvathan, personal communication.
21 R. Mason, K.M. Thomas and D.M.P. Mingos, J. Am. Chem. Soc., 95 (1973) 3802; M. McPartlin, C.R. Eady, F.G. Johnson and J. Lewis, J. Chem. Soc., Chem. Commun., (1976) 883.
22 S.W. Feldberg in A.J. Bard (Ed.), 'Electroanalytical Chemistry', Vol. 3, Marcel Dekker, New York, 1969, p. 199.
23 A.J. Bard and L.R. Faulkner, 'Electron Methods, Fundamentals and Application', Wiley, New York, 1980, p. 238.
24 L. Nadjo and J.M. Saveant, J. Electroanal. Chem., 48 (1973) 113.
25 J.L. Graff, R.D. Sanner and M.S. Wrighton, J. Am. Chem. Soc., 101 (1979) 273; D.R. Tyler, M. Altobelli and H.B. Gray, J. Am. Chem. Soc., 102 (1980) 3022.
26 J.W. Kelland and J.R. Norton, J. Organomet. Chem., 149 (1978) 185.
27 N. Cook, L. Smart and P. Woodward, J. Chem. Soc., Dalton Trans., (1977) 1744.
28 F.W.B. Einstein, S. Nussbaum, D. Sutton and A.C. Wills, Organometallics, 2 (1983) 1259.
29 J.R. Norton, J.P. Collman, G. Dolcetti and W.T. Robinson, Inorg. Chem., 11 (1972) 382.
30 S.K. Malik and A. Poe, Inorg. Chem., 17 (1978) 1484.
31 D. Mani and H. Vahrenkamp, Angew. Chem. Int. Ed. Engl., 24 (1985) 425.
32 A. Martinsen and J. Songstadt, Acta. Chem. Scand. Ser. A., A31 (1977) 645.
33 A.J. McQuillan, University of Otago, unpublished work.
34 C.C. Nagel, J.C. Bricker, D.G. Alway and S.G. Shore, J. Organomet. Chem., 219 (1981) C9; C.T. Hayward and J.R. Shapley, Inorg. Chem., 21 (1982) 3816.
35 B.M. Peake, B.H. Robinson, J. Simpson and D.J. Watson, Inorg. Chem., 16 (1979) 405.
36 A.J. Downard, B.H. Robinson and J. Simpson, Organometallics, 5 (1986) 1132.